JOURNAL OF VIROLOGY, June 1993, p. 3142–3150
0022-538X/93/063142-09$02.00/0

Vol. 67, No. 6

Human Papillomavirus Type 18 E7 Protein Requires Intact Cys-X-X-Cys Motifs for Zinc Binding, Dimerization, and Transformation but Not for Rb Binding

MARITZA C. McINTYRE,[1] MARK G. FRATTINI,[2] STEVEN R. GROSSMAN,[3]† AND LAIMONIS A. LAIMINS[1,4]*

Committee on Virology,[1] Department of Biochemistry and Molecular Biology,[2] Howard Hughes Medical Institute,[4] and Department of Molecular Genetics and Cell Biology,[3] The University of Chicago, Chicago, Illinois 60637

Received 12 October 1992/Accepted 3 March 1993

Human papillomavirus type 18 (HPV-18) E7 proteins bind zinc through Cys-X-X-Cys repeats located at the C terminus of the protein. In order to examine the role of these cysteine motifs in E7 function, we expressed the HPV-18 E7 protein in bacteria and found that purified E7 forms a dimer through interactions with zinc. Mutants with single mutations within the Cys-X-X-Cys motifs bound a reduced level of zinc in a zinc blot assay, while a double mutant lost all zinc-binding activity. When expressed in vivo, none of the mutants cooperated with an activated *ras* oncogene to transform primary rat embryo fibroblasts, but all mutants retained nearly wild-type Rb-binding activity. The results indicate that the cysteine motifs play an important role in transformation by HPV-18 E7 but do not contribute to Rb binding.

The E6 and E7 genes of human papillomavirus types 16 (HPV-16), HPV-18, and HPV-31 are selectively retained and expressed in cervical carcinomas (1, 7, 12, 13, 27, 31, 39–41). The E7 gene product can independently transform immortalized rodent cells as well as primary rat embryo fibroblasts (REFs) in cooperation with an activated *ras* oncogene (4, 8, 9, 15, 23, 24, 28, 43, 44). The E6 gene can also transform immortalized rodent cells and is required in conjunction with E7 for the high-frequency transformation of human keratinocytes, the natural host for HPV infection (3, 21, 22, 25, 29, 35, 38, 45). These studies thus implicate E6 and E7 as viral oncogenes.

The HPV-18 E7 gene encodes a protein of 105 amino acids which, like the adenovirus E1a oncoprotein and simian virus 40 (SV40) large T antigen, can bind the retinoblastoma gene product (Rb) (14, 18, 32). In addition, E7, like E1a, transactivates the adenovirus E2 promoter and binds zinc (2, 10, 34). A region of homology to conserved regions 1 and 2 (CR1 and CR2) of adenovirus E1a and SV40 large T antigen is present in the amino terminus (amino acids 2 to 43) of HPV-18 E7 (Fig. 1). The CR2 domain has been shown to mediate the association of these oncoproteins with Rb. Mutations that affect Rb binding also abolish the transformation ability of these proteins (15, 18, 20, 22, 34, 44). Thus, inhibition of the growth-regulatory function of Rb is believed to be part of the mechanism by which E1a, SV40 large T antigen, and E7 bring about a transformed phenotype.

All HPV E7 proteins have another region of homology within their carboxy termini, consisting of two Cys-X-X-Cys motifs spaced 29 amino acids apart (Fig. 1). HPV-16 E7 peptides containing one or both of these motifs can bind zinc and transactivate the adenovirus E2 promoter (36). Furthermore, HPV-16 mutants carrying mutations within the Cys-X-X-Cys motifs exhibit reduced ability to transform a variety of rodent fibroblasts, fail to immortalize human keratinocytes, and exhibit lower transactivating efficiency (15, 22, 44). These data suggest that the zinc-binding region of the E7 proteins is an important functional domain.

Although the abilities to bind zinc and transactivate are indicative of a DNA-binding protein, no such activity has been demonstrated for E7. Moreover, the structure and positioning of the zinc-binding motifs are not typical of zinc finger DNA-binding domains defined in proteins with known DNA-binding activity (5, 6). Another role for zinc binding could be to mediate multimerization of monomeric subunits. The human immunodeficiency virus Tat protein and human growth hormone have each been shown to form metal-linked dimers (11, 16, 17). Similarly, the T4D bacteriophage gene product 12, a tail fiber protein, forms a trimer through interactions with zinc (46). Thus, it seemed possible that zinc could play a similar role in E7. Previous studies with glycerol gradient fractionation of HPV-16 E7 expressed transiently in Cos cells suggest that the protein may exist in a multimeric complex with itself or with cellular proteins (42). In addition, bacterially synthesized HPV-16 E7 protein has been observed to elute as a species that is larger than its estimated molecular weight after size exclusion chromatography (33).

In this study, we show that HPV-18 E7 expressed in bacteria exists as a dimer whose formation is sensitive to chelation of zinc. We also demonstrate that mutations within the zinc-binding motifs result in the reduced ability of E7 to bind ^{65}Zn and transform REFs. Interestingly, the ability to bind Rb is not affected by these mutations.

MATERIALS AND METHODS

Plasmids. HPV-18 E7 sequences were generated by polymerase chain reaction (PCR) from plasmid HPV-18 1.5 (4) and cloned into the bacterial expression vector pET8c (42b) to create pETE7. Synthetic oligonucleotides to E7 were generated so that an *Nco*I site was added to the 5′ end of the gene and a *Bam*HI site was created at the 3′ end during amplification. The *Nco*I site contains an ATG which serves as the translation initiation start for the E7 protein. Because

* Corresponding author.
† Present address: Department of Medicine, Brigham and Women's Hospital, Boston, MA 02155.

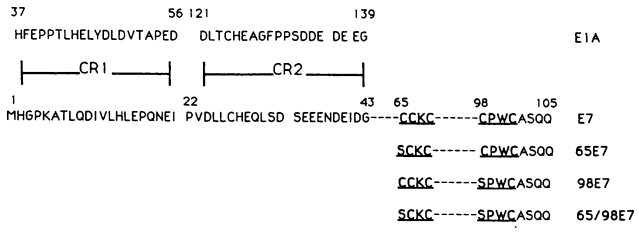

FIG. 1. Conserved regions between adenovirus E1A and HPV-18 E7 proteins, indicated by CR1 and CR2. Cys-X-X-Cys motifs are shown in boldface type. Point mutations changing cysteine residues to serine residues are indicated for each E7 mutant.

of the recognition sequence for *Nco*I, an extra GC exists between the first Met and amino acid number 2 of E7. Thus, to keep the protein-coding sequence in frame, a T was added to the PCR primer between the *Nco*I site and the coding sequence of E7, resulting in the insertion of a GCT codon (Ala) between the start codon and amino acid number 2 of the protein. E7 was also cloned into the bacterial expression vector pEX2 (42a) at the *Sma*I and *Xba*I sites by digesting HPV-18 1.5 with *Ssp*I and *Xba*I. The resultant construct, pEXE7, expresses a β-galactosidase-E7 fusion protein.

E7 mutants were generated from plasmid pSG18E7 (26) by using internal primers which differed from the wild-type sequence by 1 bp. In this way, pS65C2SE7 and pS98C2SE7, in which cysteines 65 and 98, respectively, are changed to serine, were generated and cloned into the eukaryotic expression vector pSG5. The double mutant pS6598C2SE7 was constructed by digesting the respective single mutants with *Pvu*II, isolating the mutated E7-containing sequences, and ligating them.

Mutant E7 genes were put under the control of HPV-18 regulatory sequences by cloning the mutant forms of E7 into plasmid p18PEpolyA (4). Wild-type or mutant E7 sequences and the adjacent poly(A) sequences were isolated from the pSG5 plasmids by digestion with *Nsi*I and *Xba*I. These sequences were ligated into p18PEpolyA at the *Nsi*I and *Eco*RI sites to create p18PE7, p18P65E7, p18P98E7, and p18P65/98E7. The *Xba*I and *Eco*RI sites were filled in with Klenow fragment to create blunt ends. E7 mutants were also inserted into the bacterial expression vector pET8c by digesting the pSG5 clones with *Ban*II and *Bgl*II and ligating to *Ban*II-digested pETE7 to create pET65C2SE7, pET98C2SE7, and pET65/98C2SE7. PCR-generated sequences were verified by sequencing.

Antibodies. Anti-Rb antibody Rb-PMG-245 and the immunoglobulin G1(κ) [IgG1(κ)] isotype control antibody were obtained from Pharmingen. β-Galactosidase-E7 fusion protein was expressed and purified as described before (42a) and used to immunize rabbits. Polyclonal β-gal-E7 antibody 1041 was affinity purified by using purified bacterial E7 linked to cyanogen bromide-activated Sepharose to yield affE7. Unpurified antibody 1041 was used in Western immunoblots, and affE7 was used for immunoprecipitations.

***Escherichia coli* expression and purification of wild-type HPV-18 E7.** pETE7 gene expression is under the control of the T7 gene promoter, which requires T7 RNA polymerase for transcription. The pETE7 expression plasmids were transformed into pLysS/DE3 lysogens (42b), which contain an inducible T7 RNA polymerase gene. Wild-type E7-containing cultures were grown at 37°C to mid-log phase (optical density at 550 nm of 0.5) and induced to express E7 with 0.4 mM isopropyl-1-thio-β-galactopyranoside (IPTG). Cells were harvested at 2 h postinduction, pelleted, resuspended in 50 mM Tris (pH 8.0)–2 mM EDTA–10 μM $ZnCl_2$–1 mM dithiothreitol (DTT) and frozen. Cells were lysed by freeze-thawing, and insoluble material was removed by centrifugation at 100,000 × *g*. E7 was precipitated from the soluble material by the addition of 35% ammonium sulfate, resuspended in buffer Q (25 mM Tris, 100 mM NaCl, 10 μM $ZnCl_2$, 1 mM DTT [pH 7.5]) and dialyzed against the same buffer. Dialyzed protein was loaded onto a MonoQ anion-exchange column (Pharmacia) in buffer Q, and bound proteins were eluted with a 20-ml 100 to 600 mM NaCl gradient, with E7 eluting at 400 to 430 mM NaCl. E7-containing fractions were pooled, concentrated with a Centricon microconcentrator (Amicon), and loaded onto a Superdex-75 gel filtration column (Pharmacia) equilibrated with buffer G (25 mM Tris, 150 mM NaCl, 10 μM $ZnCl_2$, 1 mM DTT). Gel filtration fractions corresponding to the E7 peak were run for 15 h at 4°C on a 15 to 25% polyacrylamide (acrylamide-bisacrylamide, 29:1) nondenaturing gradient gel which had been prerun to remove ammonium persulfate. Nondenaturing gel running buffer (27.5 mM Tris, 211 mM glycine) contained 10 μM $ZnCl_2$ to prevent the loss of zinc ions during polyacrylamide gel electrophoresis (PAGE). Gels were stained with Coomassie brilliant blue R-250 (Sigma) to visualize proteins.

Effects of EDTA on multimerization. Purified E7 protein (5 μg) was diluted in a final volume of 50 μl with buffer containing 25 mM Tris, 150 mM NaCl, 4 M urea, and 1 mM DTT; 25 mM EDTA was added, and the samples were either heated to 80°C for 5 min or left on ice. The heated samples were allowed to slowly cool to room temperature in a water bath. When the samples had cooled to 50°C, 0.5 mM $ZnCl_2$ was added to one EDTA-containing sample in the water bath and to one EDTA-containing sample on ice. Once the heated samples had reached room temperature, all samples were electrophoresed on a 15 to 25% nondenaturing gel as described above. Protein was visualized by staining with Coomassie brilliant blue G-250 (Sigma). The same experiment was performed with 25 mM ethylene glycol tetraacetic acid (EGTA) instead of EDTA as a control for zinc specificity.

To monitor the appearance of faster-migrating species after chelation by zinc, 5 μg of E7 protein was diluted in buffer as above, and either 100 or 10 mM EDTA was added. Samples were incubated on ice for from 30 min to 4 h and then electrophoresed as described above. Proteins were transferred to nitrocellulose (Schleicher and Schuell) and detected by Western blot with polyclonal anti-E7 antibody 1041 and alkaline phosphatase-conjugated goat anti-rabbit immunoglobulin as the second antibody (Bio-Rad Laboratories).

Zinc blot of wild-type and mutant E7 proteins. Zinc binding was assayed as reported before (2, 19, 37). Briefly, bacterial expression of wild-type or mutant E7 was induced as described above. Then, 1 ml of wild-type or mutant E7-expressing bacteria was pelleted, resuspended in sample buffer, and run on a 15% polyacrylamide gel with sodium dodecyl sulfate (SDS). Uninduced bacteria (1 ml) containing wild-type or mutant E7 constructs was also run as a control. Proteins were transferred to an Immobilon P (Millipore Corp.) filter and incubated in renaturing buffer (100 mM Tris, 50 mM NaCl, 10 mM DTT [pH 6.8]). The filters were then rinsed twice in labeling buffer (100 mM Tris, 50 mM NaCl [pH 6.8]) and reacted with $^{65}ZnCl_2$ (Amersham) at a concentration of 15 μM in labeling buffer for 15 min. Finally, the filters were washed in wash buffer (100 mM Tris, 50 mM

NaCl, 1 mM DTT) for 1 h, allowed to air dry, and exposed by autoradiography. Zinc binding was quantitated by scanning densitometry. To ensure that equal levels of wild-type and mutant E7 were present, proteins were visualized by Western blot as described above.

Cells and transfections. Primary REFs (Whitaker) were grown in Dulbecco's modified Eagle's medium (JRH Biosciences) supplemented with 10% fetal bovine serum (GIBCO). Cells (10^6) were transfected as described previously (4) with 55 μg of total DNA. After selection for G418-resistant colonies, the plates were stained with Giemsa stain and scored for the presence of transformed colonies.

Cos-7 cells were grown in Dulbecco's modified Eagle's medium (JRH Biosciences) supplemented with 10% calf serum (GIBCO). Cells (10^6) were transfected with 10 μg of test plasmid DNA, plated in 10 ml of medium, and harvested 40 h later for immunoprecipitation.

Immunoprecipitation. Transfected Cos-7 cells were starved in cysteine-free minimal essential medium (GIBCO) for 1 h and then labeled for 3 h with 0.5 mCi of [^{35}S]cysteine (ICN). Cells were lysed in ELB lysis buffer as described before (18) and cleared with normal rabbit serum. Sample sizes were normalized by equal amounts of trichloroacetic acid-precipitable counts and mixed with either affE7, Rb-PMG-245, or IgG1(κ) isotype control antibodies for 1 h. The anti-Rb and isotype control antibody-containing samples were mixed with a secondary rabbit anti-mouse IgG antibody after 30 min. Immune complexes were then precipitated with protein A-Sepharose (Pharmacia), washed four times in ELB, resuspended in sample buffer, and electrophoresed on a 12% polyacrylamide–SDS gel. The gel was fixed, soaked in Amplify (Amersham), dried, and visualized by fluorography. Radioactive E7 protein coprecipitated by anti-Rb antibody was quantified by Betascope analysis (Betagen). The amount of radioactivity determined for wild-type E7 was assigned a value of 100%, and the amount of mutant E7 protein coprecipitated with Rb was compared with this value. The values given represent averages for several experiments.

In vitro translation and association of E7 and Rb. Wild-type and mutant E7 sequences in pSG5 were transcribed in vitro with T7 RNA polymerase (Stratagene). The proteins were translated in wheat germ extract (Promega) and labeled with [^{35}S]cysteine. An Rb cDNA clone in pSG5 (kindly provided by Dennis McCance) was transcribed and translated in a TNT-coupled reticulocyte lysate extract (Promega) with T7 RNA polymerase. Rb protein was labeled with [^{35}S]methionine. The translation products were mixed for 2 h at 4°C in ELB buffer, and the reaction mixes were divided in half and mixed with anti-E7 or anti-Rb antibodies as described above. Immune complexes were precipitated with protein A-Sepharose and washed as described above. Proteins were electrophoresed on a 12% polyacrylamide–SDS gel and visualized by fluorography.

Determination of protein half-life. For pulse-chase analysis of wild-type and mutant E7 proteins, Cos-7 cells were transfected as above and pulse labeled for 1 h. Cells were either harvested immediately after the pulse or washed with phosphate-buffered saline (PBS) and incubated in chase medium containing excess unlabeled cysteine for 1 or 3 h. Proteins were immunoprecipitated, electrophoresed, and visualized as described above. Proteins were quantitated by Betascope analysis.

Detection of wild-type and mutant E7 by indirect immunofluorescence staining. Cos-7 cells were transfected with wild-type or mutant E7 as above and plated at a low density on chamber slides (Nunc). At 40 h after transfection, cells were washed with PBS and fixed in periodate-lysine-paraformaldehyde fixative (30). After a 30-min wash in PBS, cells were incubated with affE7 antibodies for 30 min at 25°C, washed in PBS, and incubated for a further 30 min with fluorescein isothiocyanate-conjugated goat anti-rabbit IgG (Amersham).

RESULTS

Purification of HPV-18 E7. To study the biochemical properties of the E7 protein of HPV-18, we expressed the E7 open reading frame under the control of an inducible T7 promoter in *E. coli*. In the vector pETE7, E7 is synthesized from its own translation initiation codon and migrates as a 14-kDa band on denaturing gels, although its predicted molecular mass is 12 kDa. Similar observations of aberrant migration on denaturing gels have been made for HPV-16 E7, HPV-18 E7, and bovine papillomavirus type 1 E7 (2, 42).

After induction of E7 expression, the cells were lysed and subjected to high-speed centrifugation. Over 50% of the total E7 protein was found in the soluble supernatant fraction (Fig. 2A). This soluble E7 was partially purified by ammonium sulfate precipitation and ion-exchange chromatography. E7-containing fractions were then pooled, concentrated, and loaded onto a gel filtration column. Pure E7 proteins eluted from this column in two peaks, one migrating between bovine serum albumin (BSA) and ovalbumin, and the other migrating between carbonic anhydrase and α-lactalbumin. This elution pattern suggested that E7 was associated into forms larger than monomers. After addition of 10 μM $ZnCl_2$ to our buffers, the protein eluted in a single peak corresponding to the larger-molecular-weight complex (Fig. 2B). This observation indicates that E7 proteins associate as multimers and suggests a role for zinc in this association.

To more accurately characterize the size of these E7 complexes, we ran the gel filtration fractions on nondenaturing gels. Initial results yielded protein which migrated at various sizes, which ranged from four times the molecular weight or larger to species that corresponded to monomers. We suspected that this variation in size could be the result of aggregation of the protein due to oxidation and loss of zinc ions during electrophoresis. Therefore, gels were prerun to remove ammonium persulfate, and 10 μM $ZnCl_2$ was added to the running buffer to prevent loss of zinc during electrophoresis. Under these conditions, all gel filtration fractions were observed to migrate as a single species (Fig. 2C). Compared with proteins with similar isoelectric points (pIs) (4.9, 4.6, and 5.3 for BSA, ovalbumin, and α-lactalbumin, respectively; the estimated pI of HPV-18 E7 is 4.9), the size of the E7 complex was estimated to be approximately 28 kDa, or twice the size of monomeric E7.

While both gel filtration and nondenaturing gel electrophoresis analysis demonstrated that E7 proteins form multimeric complexes, the former suggested that these complexes were tetramers, while the latter suggested that E7 exists as a dimer. It was possible that E7 forms tetrameric complexes at high protein concentrations but dissociates to a dimer upon dilution during gel filtration. Therefore, we examined the concentration dependence of E7 multimer formation by reapplying purified, dilute E7 protein to the sizing column. E7 eluted as a single complex with the same size as the concentrated protein (not shown). Additionally, when an aliquot of partially purified, concentrated E7 was removed before being loaded onto the gel filtration column and run on a nondenaturing gel, it migrated as a species of the same size as the eluted gel filtration fractions (Fig. 2C, lane 4). These

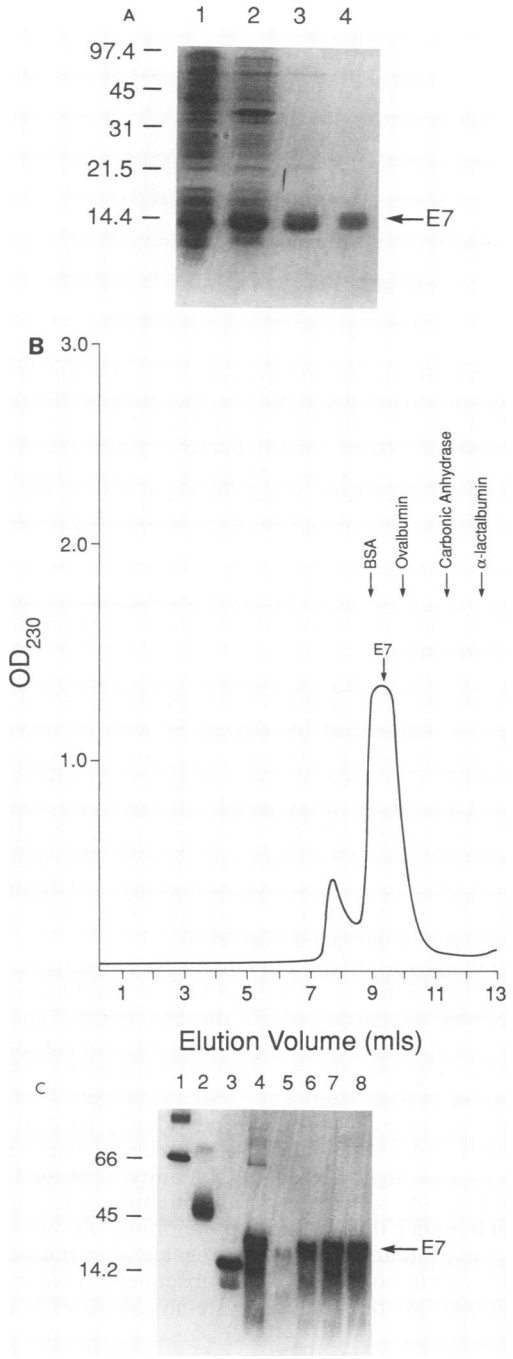

FIG. 2. Purification and size determination of HPV-18 E7 protein. (A) SDS–15% polyacrylamide gel of bacterially expressed E7. Numbers at left indicate the size (in kilodaltons) of nonstained markers. E7 is indicated at right. Lane 1, soluble E7-expressing bacterial lysate; lane 2, insoluble bacterial lysate in 8 M urea; lane 3, pooled MonoQ eluate; lane 4, Superdex-75 eluate pool. (B) Elution profile of E7. Partially purified E7 was loaded onto a calibrated Superdex-75 gel filtration column, and eluted fractions were analyzed by SDS-PAGE. The E7 elution peak is marked with an arrow. The standards used to calibrate the column were BSA (66 kDa), ovalbumin (45 kDa), carbonic anhydrase (29 kDa), and α-lactalbumin (14.2 kDa). Their elution volumes are indicated. (C) Nondenaturing gel electrophoresis of purified E7. Fractions corresponding to the E7 peak (fractions 37 to 40) were run on a 15 to 25% polyacrylamide nondenaturing gel, and the sizes of the complexes were determined (lanes 5 to 8, respectively). E7 protein is indicated at right (arrow). Lanes 1 to 3, size markers (BSA, ovalbumin, and α-lactalbumin). Sizes are indicated at the left (in kilodaltons). Lane 4, pooled and concentrated MonoQ eluate. Proteins were visualized by Coomassie staining.

results suggest that the complexes observed on gel filtration and nondenaturing gels are not different-sized complexes but indicate inaccuracy in one of the methods used to estimate molecular weight.

While gel filtration is a commonly used technique for the determination of the molecular weight of proteins, the procedure is limited by the need to use protein standards of the same shape as the protein of interest in the calibration of the column (25a). The standards used to calibrate the column are all of a globular nature. Given the predicted mechanism by which E7 coordinates zinc through the carboxy-terminal Cys-X-X-Cys motifs, it is possible that E7 does not fold into a compact protein (2, 33, 36). Thus, its behavior on a gel filtration column may not be properly reflected by the standards used to calibrate the column. Alternatively, nondenaturing gel electrophoresis is influenced more by the charge and mass of the proteins under the given buffer conditions than by shape (25a). Since all of the standards and E7 are negatively charged under the buffer conditions used (pH 8.3), nondenaturing gel electrophoresis is likely to be a more accurate method for determination of the molecular weight of the E7 complex. Thus, we conclude that E7 exists as a dimer.

Effects of zinc chelation on E7 multimerization. The influence of zinc on the elution profile of E7 from the gel filtration column suggested that this metal ion could play an important role in the association of E7 into multimers. The role of zinc in the oligomerization of E7 was examined through the use of the metal-chelating compound EDTA. When EDTA was added to a purified preparation of E7 at 4°C, very little change in dimer formation was observed, as determined by nondenaturing gel electrophoresis (data not shown). One explanation for this result is that the zinc ions are buried by protein folding and thus inaccessible to EDTA. We therefore investigated whether unfolding by heating in the presence of EDTA and refolding through slow cooling could affect the reformation of multimeric E7.

When purified E7 was heated to 85°C in the absence of EDTA and then allowed to cool, it was observed to readily reassociate to form dimeric proteins identical to the starting material. In contrast, addition of EDTA during unfolding at high temperature and subsequent cooling led to the formation of high-molecular-weight aggregates which were unable to migrate into the gel. These results indicated that proper refolding of E7 was inhibited by the absence of zinc (not shown).

To prevent aggregation after chelation of zinc, experiments were next performed in the presence of 4 M urea, which does not affect multimer formation in the absence of EDTA (Fig. 3, lanes 1 and 4). When EDTA was added to E7 protein in the presence of urea at 4°C, two novel forms, in addition to the dimeric form of E7, were consistently observed (Fig. 3, lane 2). These two newly observed species migrated faster than the E7 dimer, but their migration pattern could be reversed to the dimeric state by the addition of $ZnCl_2$ to the reaction mix (Fig. 3, lane 3). When similar samples containing urea were heated and allowed to cool slowly, the addition of EDTA led to the appearance of only the two novel species observed above; no dimeric E7 was

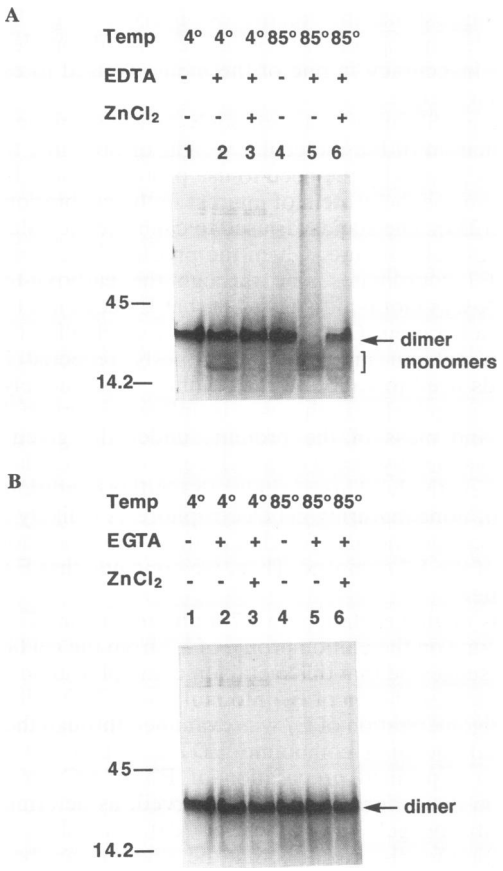

FIG. 3. (A) EDTA treatment of purified E7 in the presence of 4 M urea. Lanes 1 and 4, control samples of purified E7 without EDTA; lanes 2, 3, 5, and 6, 5 μg of purified E7 treated with 25 mM EDTA as described in Materials and Methods and either left on ice (lanes 1, 2, and 3) or heated to 85°C and slowly cooled (lanes 4, 5, and 6). When heated samples had cooled to 50°C, 0.5 mM $ZnCl_2$ was added to the samples in lanes 3 and 6. Samples were run on a nondenaturing gel, and proteins were visualized by staining with Coomassie brilliant blue G-250. The positions of ovalbumin (45 kDa) and α-lactalbumin (14.2 kDa) are indicated at left. The migration patterns of dimeric and monomeric E7 are indicated at right. (B) Experiment using EGTA instead of EDTA.

observed (Fig. 3, lane 5). A smear along the length of the lane was also apparent, suggesting that a portion of the protein still aggregates upon chelation of zinc, even in the presence of 4 M urea. However, the addition of 0.5 mM $ZnCl_2$ to EDTA-treated samples during refolding led to the reappearance of the dimeric form of E7 (Fig. 3, lane 6) and a decrease in the monomeric forms as well as the high-molecular-weight aggregates. These observations demonstrate the role of zinc in the formation of E7 dimers. When EGTA was used in a similar experiment, no change in migration was observed even after heating to 85°C (Fig. 3B), due to the 100-fold-lower affinity of EGTA than of EDTA for zinc (7a).

In order to rule out the possibility that disulfide bonding contributed to dimerization, E7 protein samples were incubated in the presence of increasing amounts of DTT (0.5 to 10 mM) and run on a nondenaturing gel. No change in the mobility of the protein was observed under these conditions (data not shown). We therefore conclude that the formation

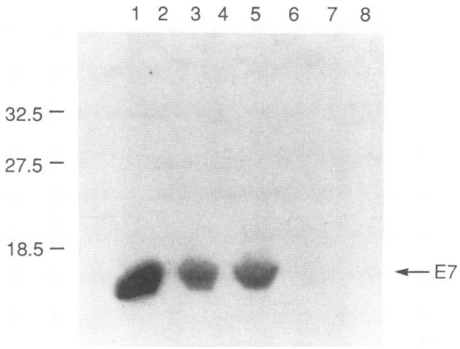

FIG. 4. Zinc binding by wild-type and mutant E7 proteins. Zinc blot of induced and uninduced bacteria containing pETE7 (lanes 1 and 2), pET65C2SE7 (lanes 3 and 4), pET98C2SE7 (lanes 5 and 6), and pET65/98C2SE7 (lanes 7 and 8). Bacterial lysates were run on a 15% polyacrylamide–SDS gel, transferred to Immobilon P, and incubated with 15 μM $^{65}ZnCl_2$ as described elsewhere (2, 19). Bands were visualized by autoradiography. Sizes are shown in kilodaltons.

of dimeric complexes of E7 proteins requires only coordination of zinc ions and is not dependent on intermolecular disulfide formation.

We questioned the appearance of the two faster-migrating species upon chelation of zinc. Since migration on nondenaturing gels is influenced by charge as well as mass, we reasoned that one of the species could represent monomeric protein which still bound zinc, while the other species represented monomer from which all zinc had been removed. However, even in the presence of 100 mM EDTA, both bands still appeared (data not shown). We therefore believe that the two species represent either two differently folded species of monomer or that the lower species may represent partially degraded monomer.

Zinc binding by wild-type and mutant E7 proteins. We next investigated the effects of zinc binding on the biochemical and functional properties of E7 through genetic analysis. Coordination of zinc by E7 has been shown to occur through the cysteine motifs located at the C terminus of E7 (33, 36). We therefore mutagenized one cysteine in each Cys-X-X-Cys motif (amino acid 65 or 98) individually as well as in combination and expressed these proteins in bacteria. In contrast to the high degree of solubility observed with wild-type E7, both single and double mutants were found to be insoluble under the purification conditions described. In addition, the proteins remained aggregated after purification under denaturing conditions and subsequent renaturation, indicating that loss of even one cysteine can severely affect protein folding.

Since we were unable to determine whether mutant E7 proteins formed dimers because of their insolubility, we next examined their ability to bind zinc in a zinc blot assay. We and others have previously used this assay to examine the ability of HPV proteins to bind zinc (2, 19, 36). In this assay, bacterially expressed proteins are separated electrophoretically under denaturing conditions, transferred to a membrane support, allowed to renature, and incubated with $^{65}ZnCl_2$. The single cysteine mutants (pET65C2SE7 and pET98C2SE7) were found to bind zinc at approximately 50% of the level observed for wild-type E7, as determined by densitometry. In contrast, the double mutant (pET65/98C2SE7) exhibited no detectable zinc-binding activity (Fig. 4). No zinc-binding activity was observed in the lanes containing uninduced bacteria. Western blot analysis con-

TABLE 1. Transformation of REFs with wild-type and mutant E7-expressing constructs[a]

Plasmid(s)	No. of morphologically transformed colonies[b] in expt:		
	1	2	3
p18PEpolyA + pEJras	55	16	53
p18PE7 + pEJras	57	10	25
p18P65E7 + pEJras	0	0	0
p18P98E7 + pEJras	0	0	0
p18P65/98E7 + pEJras	0	0	0
pEJras	0	0	0
pRSVneo	0	0	0

[a] All transfections included pRSVneo.
[b] Scored by Giemsa staining.

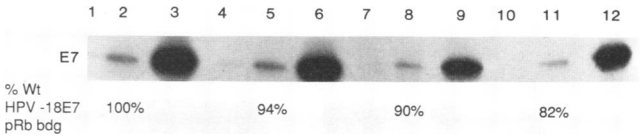

FIG. 5. Coimmunoprecipitation of Rb and wild-type or mutant E7 in Cos-7 cells transiently transfected with pSG18E7 (lanes 1 to 3), pS65C2SE7 (lanes 4 to 6), pS98C2SE7 (lanes 7 to 9), or pS6598C2SE7 (lanes 10 to 12). Cells were labeled with [^{35}S]cysteine and immunoprecipitated with control antibody IgG1(κ) (lanes 1, 4, 7, and 10), Rb-PMG-245 (lanes 2, 5, 8, and 11), or affE7 (lanes 3, 6, 9, and 12). Samples were run on a 12% polyacrylamide gel and visualized by fluorography. The amount of E7 coprecipitated by anti-Rb antibodies was determined by Betascope analysis. The percentage of wild-type (wt) binding (bdg) shown reflects the average of two experiments.

firmed that there were equal amounts of E7 protein in all lanes and no wild-type or mutant E7 protein in the uninduced-sample lanes (not shown). The fact that single cysteine mutants retained appreciable but reduced zinc-binding ability suggests that zinc binding can still occur between the remaining intact Cys-X-X-Cys motifs of single-mutant protein subunits.

Transformation of REFs. Wild-type and E7 mutants were next tested for their ability to cooperate with an activated *ras* oncogene to transform REFs. High-level expression of E7 proteins from a strong eukaryotic promoter (SV40) was toxic to cells. Since E7 has been observed to transform REFs when expressed within the context of the HPV genome, wild-type and mutant E7 proteins were cloned into a vector which expresses both the E6 and E7 genes from the homologous HPV-18 upstream regulatory region (p18PEpolyA) (4). REFs were transfected with wild-type or mutant E7-containing constructs together with pEJras and pSV2neo. Plasmid p18PEpolyA was used as a positive control. After selection with G418, plates were stained with Giemsa stain and scored for the presence of transformed colonies. The results are presented in Table 1. Wild-type E7 (p18PEpolyA and p18PE7) cooperated with *ras* to transform REFs. However, no transformed colonies were observed with either the single or double cysteine mutants (p18P65E7, p18P98E7, or p18P65/98E7). These results demonstrate that intact zinc-binding motifs within the carboxy-terminal domain of E7 are required to maintain the transforming ability of the protein.

E7 cysteine mutants bind the retinoblastoma protein as efficiently as wild-type E7. One possibility for the inability of the E7 cysteine mutants to transform REFs was a reduction in Rb-binding ability. We therefore examined these proteins for their ability to bind Rb when transiently expressed in Cos-7 cells. Wild-type E7 protein has been shown to bind Rb in Cos-7 cells in transient-expression assays (18). Wild-type or mutant E7 constructs under the control of the SV40 early promoter (pSG18E7, pS65C2SE7, pS98C2SE7, or pS6598C2SE7) were transfected into Cos-7 cells by electroporation. At 40 h posttransfection, the cells were labeled with [^{35}S]cysteine, and E7 and Rb complexes were immunoprecipitated and visualized on SDS-polyacrylamide gels. The anti-Rb antibody coprecipitated wild-type and mutant E7 proteins with relatively equal efficiency, as quantitated by Betascope analysis. No E7 proteins were observed in control precipitations with an IgG1(κ) isotype control (Fig. 5). These results suggest that E7 proteins that are reduced or deficient in the ability to bind zinc retain wild-type Rb-binding activity.

Anti-E7 antibodies were less efficient at coprecipitating Rb with either wild-type or mutant E7, which may be the result of interference with Rb-E7 interactions by the anti-E7 antibody (not shown). Thus, to ensure that the E7 precipitated by the anti-Rb antibodies was not due to nonspecific binding of E7 to the antibody, the association between Rb and wild-type or mutant E7 was tested in vitro. When Rb and E7 proteins were translated in vitro and mixed, both wild-type and mutant E7 protein was coprecipitated with Rb with either anti-E7 (Fig. 6A) or anti-Rb (Fig. 6B) antibodies. Alternatively, anti-Rb antibodies did not precipitate either wild-type or mutant E7 proteins mixed with an unprogrammed lysate, nor did anti-E7 antibodies precipitate Rb protein which had been mixed with unprogrammed lysate (Fig. 6C). Thus, the results of the transient transfection show that the cysteine mutants retain nearly wild-type Rb-binding activity.

Half-lives of E7 cysteine mutants. Another possible explanation for the loss of transformation ability by the mutant E7 proteins was a reduction in their half-life. Previous studies with a mutant E7 protein from HPV-16 suggest that mutations in one of the Cys-X-X-Cys motifs result in a decreased protein half-life (44). In order to investigate the role of each Cys-X-X-Cys motif in protein stability, the half-lives of the single and double cysteine mutant E7 proteins were determined in transiently transfected Cos cells. Cells were electroporated and pulse labeled for 1 h at 40 h posttransfection. E7 proteins were immunoprecipitated following the chase with unlabeled cysteine and examined by SDS-PAGE. Mutations in either Cys-X-X-Cys motif resulted in a shorter half-life than that of wild-type E7, while the double mutant appeared to have a half-life longer than that of wild-type E7 (Fig. 7). We determined the half-life of wild-type HPV-18 E7 to be approximately 2.5 h, while that of the Cys-65 E7 mutant was decreased to 1.5 h. The half-life of the Cys-98 E7 mutant decreased to less than 1 h. Mutations at both cysteines increased the stability of the protein, giving the double-mutant E7 a half-life of at least 6 h.

This difference in half-life between the single and double cysteine mutants suggests that the change in stability of the E7 protein may not be the mechanism resulting in the loss of transformation ability. In addition, indirect immunofluorescence studies of transiently transfected Cos cells show nearly equivalent levels of protein in cells containing wild-type or mutant E7 protein (data not shown). Immunofluorescence data also discount the possibility that mutations in the cysteines abolish nuclear localization, since all mutant protein was observed in the nucleus.

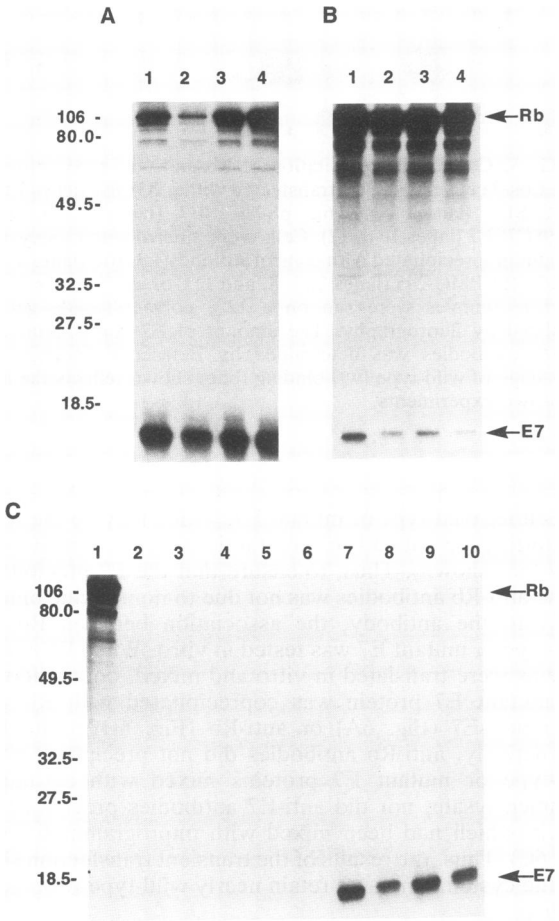

FIG. 6. Immunoprecipitation of HPV 16 E7-Rb protein complexes translated in vitro. Complexes formed between radioactively labeled wild-type or mutant E7 and Rb proteins were immunoprecipitated with affE7 antibodies (A) or Rb-PMG-245 (B). Rb was mixed with wild-type E7 (lanes 1), p65C2SE7 (lanes 2), p98C2SE7 (lanes 3), or p65/98C2SE7 (lanes 4). Panels A and B represent a 48-h exposure (A) and an 11-h exposure (B) of the same gel. (C) Immunoprecipitation of complexes formed between unprogrammed lysate and translated Rb (lanes 1 and 6), wild-type E7 (lanes 2 and 7), p65C2SE7 (lanes 3 and 8), p98C2SE7 (lanes 4 and 9), or p65/98C2SE7 (lanes 5 and 10). Anti-Rb antibody was used in lanes 1 to 5, and anti-E7 antibody was used in lanes 6 to 10. The lower levels of protein in lanes 2 in panels A and B and lane 8 in panel C are due to the lower level of labeled p65C2SE7 added to the reaction mixes and do not reflect a lower affinity for Rb protein or affE7 antibody. Sizes are shown in kilodaltons.

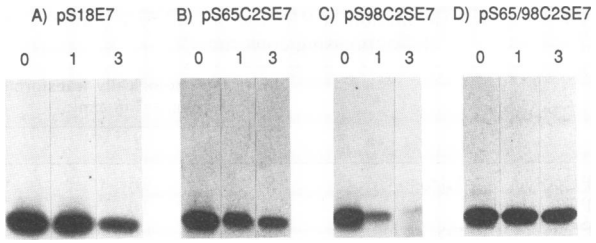

FIG. 7. Pulse-chase analysis of wild-type and mutant E7 proteins transiently expressed in Cos-7 cells. Cells were transfected with pSG18E7 (A), pS65C2SE7 (B), pS98C2SE7 (C), or pS6598C2SE7 (D). After 40 h, cells were pulsed with [^{35}S]cysteine and then either harvested immediately (lanes 0) or chased with an excess of unlabeled cysteine for 1 h (lanes 1) or 3 h (lanes 3). E7 was immunoprecipitated with affE7, separated on a 12% polyacrylamide gel, and visualized by fluorography.

DISCUSSION

In this study, we examined the influence of the Cys-X-X-Cys motifs on the multimerization and transforming ability of HPV-18 E7. We have shown that bacterially expressed, purified HPV-18 E7 protein associates into a higher-order structure, as observed by both gel filtration and nondenaturing gel electrophoresis. By nondenaturing gel electrophoresis, we determined that E7 forms dimers in solution. We have also found that zinc plays an important role in the formation of E7 dimers. Since mass spectroscopy suggests that one molecule of HPV-16 E7 binds one molecule of zinc (33), each E7 molecule could bind a single zinc atom through its two Cys-X-X-Cys motifs, or two E7 molecules could share two zinc atoms through intermolecular bonds between the Cys-X-X-Cys motifs of the two subunits (Fig. 8). Such a sharing of zinc atoms between subunits has been hypothesized for both the human immunodeficiency virus type 1 Tat protein and human growth hormone (11, 17).

This model is consistent with our observations, in which alteration of a cysteine in one Cys-X-X-Cys motif diminishes zinc binding by 50%, while mutation of a cysteine in both Cys-X-X-Cys motifs abolishes zinc binding. Such a decrease in the ability to bind zinc would be expected if each Cys-X-X-Cys motif of the protein represents half of a zinc-binding motif in conjunction with the equivalent motif on another monomeric subunit. However, mutations in both of the Cys-X-X-Cys motifs would result in total abolition of zinc binding, as we observed, since no intact zinc-binding motif could be formed either within or between the monomeric subunits of E7 protein. If each monomer were involved in coordinating one molecule of zinc, one might expect complete loss of zinc binding even with a single mutation, although the possibility exists that three active cysteines are sufficient for weak zinc binding. Additionally, observations that peptides of HPV-16 E7 containing only one Cys-X-X-Cys motif can still bind zinc in a zinc blot assay (36) strengthens the possibility that coordination of zinc by HPV E7 proteins could occur between two subunits of protein instead of within a single protein subunit. Unfortunately, further characterization of zinc coordinate structure is limited by the solubility characteristics of our present mutants.

The addition of EDTA to a preparation of purified protein resulted in the appearance of faster-migrating monomeric species on nondenaturing gels. Interestingly, two species were detected upon treatment with EDTA, both of which reverted to a single dimeric complex upon the addition of excess $ZnCl_2$, strongly suggesting that the interaction be-

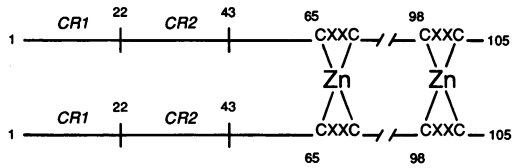

FIG. 8. Hypothetical model of dimeric HPV-18 E7 protein coordinating zinc in a parallel arrangement supported by data from cysteine mutants.

tween E7 monomers is influenced by zinc binding. While we do not have an easy explanation for the appearance of two monomeric species, we suspect that they reflect different folded states of E7. The facts that only aggregates of E7 were detected when zinc was removed in the absence of urea and that properly folded, soluble Cys-X-X-Cys mutants could not be purified are consistent with the idea that the protein requires interactions with zinc to assume its proper conformation. In the absence of zinc, or after mutation of one or more cysteine residues, the remaining cysteine residues may form nonspecific disulfide bonds either intramolecularly, resulting in monomers, or intermolecularly, resulting in aggregates. This aggregation of E7 cysteine mutants may, however, be restricted to bacterial overexpression systems. In the reducing environment of eukaryotic cells, these cysteine mutants may not be able to form intermolecular disulfide bonds and may exist as monomers. E7 proteins transiently expressed in vivo retained several biochemical properties, such as Rb binding and the ability to localize to the nucleus, suggesting that they do not form large aggregates when expressed in this system, even though they most likely are unable to bind zinc in vivo as well as in vitro.

Previous studies have shown that mutations in the cysteine motifs either significantly reduce or abolish the ability of HPV-16 E7 to transform a variety of rodent cells (15, 44). This region has similarly been shown to be required for the immortalization of primary human keratinocytes (22). We observed a complete loss of the ability to transform rodent cells with both the single and double cysteine mutants. Surprisingly, this inability to transform rodent cells in our assay does not seem to correlate with loss of retinoblastoma protein binding, since each mutant was observed to bind roughly as much Rb as wild-type E7 when transiently expressed in Cos cells. Our data as well as previous studies show that mutations in the Cys-X-X-Cys motifs alter the half-life of E7 (44). The single mutants have a decreased half-life, while the double mutant shows a longer half-life than wild-type E7. Thus, changes in transforming ability are most likely not due to half-life changes.

A possible explanation for the inability of E7 cysteine mutants to transform cells is that they are unable to dimerize because of their loss of zinc-binding ability. Dimeric E7 may be required for interaction with cellular factors other than Rb. Alternatively, dimeric E7 may be required for the release of the transcription factor E2F from E2F-Rb complexes. Recent work by Huang et al. (20a) demonstrates that while E7 CR2 peptide is capable of binding Rb, it is unable to dissociate E2F. An E7 peptide containing CR2 and at least one Cys-X-X-Cys motif was found to be required for both Rb binding and E2F dissociation. In addition, the full-length protein was much more effective in dissociating E2F complexes than the peptide containing a single Cys-X-X-Cys motif. These results indicate that E7 does not block E2F-Rb interactions merely by competition for a binding site but may act by steric hinderance. It is possible that while the intact cysteine mutants are still capable of binding Rb, the fact that they are unable to dimerize renders them incapable of blocking E2F-Rb interactions. Further experiments will be required to determine the association state of E2F in cells expressing these mutant E7 proteins.

ACKNOWLEDGMENTS

We thank Lisa Marubio and John Harlan for advice on nondenaturing gel electrophoresis. We also thank Dennis McCance, Howard Tager, Elliot Androphy, and members of the Laimins laboratory for helpful comments on the manuscript.

This work was supported by the Howard Hughes Medical Institute, a grant from the National Cancer Institute to L.A.L., and a Minority Access to Research Careers graduate fellowship to M.C.M.

REFERENCES

1. **Baker, C. C., W. C. Phelps, V. Lindgren, M. J. Braun, M. A. Gonda, and P. M. Howley.** 1987. Structural and transcriptional analysis of human papillomavirus type 16 sequences in cervical carcinoma cell lines. J. Virol. **61:**962–971.
2. **Barbosa, M. S., D. R. Lowy, and J. T. Schiller.** 1989. Papillomavirus polypeptides E6 and E7 are zinc-binding proteins. J. Virol. **63:**1404–1407.
3. **Bedell, M. A., K. H. Jones, S. R. Grossman, and L. A. Laimins.** 1989. Identification of human papillomavirus type 18 transforming genes in immortalized and primary cells. J. Virol. **63:**1247–1255.
4. **Bedell, M. A., K. H. Jones, and L. A. Laimins.** 1987. The E6-E7 region of human papillomavirus type 18 is sufficient for transformation of NIH 3T3 and Rat-1 cells. J. Virol. **61:**3635–3640.
5. **Berg, J.** 1988. Proposed structure for the zinc-binding domains from transcription factor IIIA and related proteins. Proc. Natl. Acad. Sci. USA **85:**99–102.
6. **Berg, J. M.** 1986. Potential metal-binding domains in nucleic acid binding proteins. Science **232:**485–487.
7. **Boshart, M., L. Gissmann, H. Ikenberg, A. Kleinheinz, W. Scheurlen, and H. zur Hausen.** 1984. A new type of papillomavirus DNA, its presence in genital cancer biopsies and in cell lines derived from cervical cancer. EMBO J. **3:**1151–1157.

7a. **Brown, T. A.** 1991. Molecular biology lab fax, p. 42. Bios Scientific Publishers, Oxford.

8. **Chesters, P. M., and D. J. McCance.** 1989. Human papillomavirus types 6 and 16 in cooperation with Ha-*ras* transform secondary rat embryo fibroblasts. J. Gen. Virol. **70:**353–365.
9. **Chesters, P. M., K. H. Vousden, C. Edmonds, and D. J. McCance.** 1990. Analysis of human papillomavirus type 16 open reading frame E7 immortalizing function in rat embryo fibroblast Cells. J. Gen. Virol. **71:**449–453.
10. **Culp, J. F., L. C. Webster, D. J. Friedman, C. L. Smith, W. J. Huang, Y. H. Wu, M. Rosenberg, and R. P. Ricciardi.** 1988. The 289-amino acid E1a protein of adenovirus binds zinc in a region that is important for trans-activation. Proc. Natl. Acad. Sci. USA **85:**6450–6454.
11. **Cunningham, B. C., M. G. Mulkerrin, and J. A. Wells.** 1991. Dimerization of human growth hormone by zinc. Science **253:**545–548.
12. **Durst, M., R. T. Dzarlieva-Petusevska, P. Boukamp, N. E. Fusenig, and L. Gissmann.** 1987. Molecular and cytogenetic analysis of immortalized human keratinocytes obtained after transfection with human papillomavirus type-16 DNA. Oncogene **1:**251–256.
13. **Durst, M., L. Gissmann, H. Ikenberg, and H. zur Hausen.** 1983. A papillomavirus DNA from cervical carcinoma and its prevalence in cancer biopsy samples from different geographic regions. Proc. Natl. Acad. Sci. USA **80:**3812–3815.
14. **Dyson, N., P. M. Howley, K. Munger, and E. Harlow.** 1989. The human papilloma virus-16 E7 oncoprotein is able to bind to the retinoblastoma gene product. Science **243:**934–936.
15. **Edmonds, C., and K. H. Vousden.** 1989. A point mutational analysis of human papillomavirus type 16 E7 protein. J. Virol. **63:**2650–2656.
16. **Frankel, A. D., L. Chen, R. J. Cotter, and C. O. Pabo.** 1988. Dimerization of the Tat protein from human immunodeficiency virus: a cysteine-rich peptide mimics the normal metal-linked dimer interface. Proc. Natl. Acad. Sci. USA **84:**6297–6300.
17. **Frankel, A. D., and C. O. Pabo.** 1988. Tat protein from human immunodeficiency virus forms a metal-linked dimer. Science **240:**70–73.
18. **Gage, J. R., C. Meyers, and F. O. Wettstein.** 1990. The E7 proteins of the nononcogenic human papillomavirus type 16 differ in retinoblastoma protein binding and other properties. J. Virol. **64:**723–730.
19. **Grossman, S. R., and L. A. Laimins.** 1989. E6 protein of human

papillomavirus type 18 binds zinc. Oncogene **4**:1089–1093.

20. **Heck, D. V., C. L. Yee, P. M. Howley, and K. Munger.** 1992. Efficiency of binding of the retinoblastoma protein correlates with the transforming capacity of the E7 oncoproteins of the human papillomaviruses. Proc. Natl. Acad. Sci. USA **89**:4442–4446.

20a. **Huang, P. S., D. R. Patrick, G. Edwards, P. J. Goodhart, H. E. Huber, L. Miles, V. M. Garsky, A. Oliff, and D. C. Heimbrook.** 1993. Protein domains governing interactions between E2F, the retinoblastoma gene product, and human papillomavirus type 16 E7 protein. Mol. Cell. Biol. **13**:953–960.

21. **Hudson, J. B., M. A. Bedell, D. J. McCance, and L. A. Laimins.** 1990. Immortalization and altered differentiation of human keratinocytes in vitro by the E6 and E7 open reading frames of human papillomavirus type 18. J. Virol. **64**:519–526.

22. **Jewers, R. J., P. Hildebrandt, J. W. Ludlow, B. Kell, and D. J. McCance.** 1992. Regions of human papillomavirus type 16 E7 oncoprotein required for immortalization of human keratinocytes. J. Virol. **66**:1329–1335.

23. **Kanda, T., A. Furuno, and K. Yoshiike.** 1988. Human papillomavirus type 16 open reading frame E7 encodes a transforming gene for rat 3Y1 cells. J. Virol. **62**:610–613.

24. **Kanda, T., S. Watanabe, and K. Yoshiike.** 1988. Immortalization of primary rat cells by human papillomavirus type 16 subgenomic DNA fragments controlled by the SV40 promoter. Virology **165**:321–325.

25. **Kaur, P., and J. K. McDougall.** 1988. Characterization of primary human keratinocytes transformed by human papillomavirus type 18. J. Virol. **62**:1917–1924.

25a. **Laue, T. M., and D. G. Rhodes.** 1990. Determination of size, molecular weight and presence of subunits. Methods Enzymol. **182**:566–587.

26. **Lechner, M. S., D. H. Mack, A. B. Finicle, T. Crook, K. H. Vousden, and L. A. Laimins.** 1992. Human papillomavirus E6 proteins bind p53 *in vivo* and abrogate p53-mediated repression of transcription. EMBO J. **11**:3045–3052.

27. **Lorincz, A. T., W. D. Lancaster, and G. F. Temple.** 1986. Cloning and characterization of the DNA of a new human papillomavirus from a woman with dysplasia of the uterine cervix. J. Virol. **58**:225–229.

28. **Matlashewski, G., J. Schneider, L. Banks, N. Jones, A. Murray, and L. Crawford.** 1987. Human papillomavirus type 16 DNA cooperates with activated ras in transforming primary cells. EMBO J. **6**:1741–1746.

29. **McCance, D. J., R. Kopan, E. Fuchas, and L. A. Laimins.** 1988. Human papillomavirus type 16 alters human epithelial cell differentiation *in vitro*. Proc. Natl. Acad. Sci. USA **85**:7169–7173.

30. **McLean, I. W., and P. K. Nakahe.** 1974. Periodate-lysine-paraformaldehyde fixative. A new fixative for immunoelectron microscopy. J. Histochem. Cytochem. **22**:1077–1083.

31. **McNab, J. C., S. A. Walkinshaw, J. W. Corinder, and J. B. Clements.** 1986. Human papillomavirus in clinically and histologically normal tissue of patients with genital cancer. N. Engl. J. Med. **513**:1052–1058.

32. **Munger, K., B. A. Werness, N. Dyson, W. C. Phelps, E. Harlow, and P. M. Howley.** 1989. Complex formation of human papillomavirus E7 proteins with the retinoblastoma tumor suppressor gene product. EMBO J. **8**:4099–4105.

33. **Patrick, D. R., K. Zhanf, D. Defeo-Jones, G. R. Vuocolo, R. Z. Maigetter, M. K. Sardana, A. Oliff, and D. C. Heimbrook.** 1992. Characterization of functional HPV-16 E7 proteins produced in *Escherichia coli*. J. Biol. Chem. **267**:6910–6915.

34. **Phelps, W. C., C. L. Yee, K. Munger, and P. M. Howley.** 1988. The human papillomavirus type 16 E7 gene encodes transactivation and transformation functions similar to those of adenovirus E1A. Cell **53**:539–547.

35. **Pirisi, L., S. Yasumoto, M. Feller, J. Doniger, and J. A. DiPaolo.** 1987. Transformation of human fibroblasts and keratinocytes with human papillomavirus type 16 DNA. J. Virol. **61**:1061–1066.

36. **Rawls, J. A., R. Pusztai, and M. Green.** 1990. Chemical synthesis of human papillomavirus type 16 E7 oncoprotein: autonomous protein domains for induction of cellular DNA synthesis and for *trans* activation. J. Virol. **64**:6121–6129.

37. **Schiff, L. A., M. L. Nibert, and B. N. Fields.** 1988. Characterization of a zinc blotting technique: evidence that a retroviral gag protein binds zinc. Proc. Natl. Acad. Sci. USA **85**:4195–4199.

38. **Schlegel, R., W. C. Phelps, Y. L. Zhang, and M. Barbosa.** 1988. Quantitative keratinocyte assay detects two biological activities of human papillomavirus DNA and identifies viral types associated with cervical carcinoma. EMBO J. **7**:3181–3187.

39. **Schneider-Gaedicke, A., and E. Schwarz.** 1986. Different human cervical carcinoma cell lines show similar transcription patterns of human papillomavirus early genes. EMBO J. **5**:2285–2292.

40. **Schwarz, E., U. K. Freese, L. Gissmann, W. Mayer, B. Roggenbuck, A. Stremlau, and H. zur Hausen.** 1985. Structure and transcription of human paplillomavirus sequences in cervical carcinoma cells. Nature (London) **314**:1111–1114.

41. **Smotkin, D., and F. O. Wettstein.** 1986. Transcription of human papillomavirus type 16 early genes in cervical cancer and a cancer-derived cell line and identification of the E7 protein. Proc. Natl. Acad. Sci. USA **83**:4680–4684.

42. **Smotkin, D., and F. O. Wettstein.** 1987. The major human papillomavirus protein in cervical cancers is a cytoplasmic phosphoprotein. J. Virol. **61**:1686–1689.

42a. **Stanley, K. K., and J. P. Luzio.** 1984. Construction of a new family of high efficiency bacterial expression vectors: identification of cDNA clones coding for human liver proteins. EMBO J. **3**:1492–1434.

42b. **Studier, F. W., A. H. Rosenberg, J. J. Dunn, and J. W. Dubendorf.** 1990. Use of T7 RNA polymerase to direct expression of cloned genes. Methods Enzymol. **185**:60–89.

43. **Vousden, K. H., J. Doniger, J. A. DiPaolo, and D. R. Lowy.** 1988. The E7 open reading frame of human papillomavirus type 16 encodes a transforming gene. Oncogene Res. **3**:167–175.

44. **Watanabe, S., T. Kanda, H. Sato, A. Furuno, and K. Yoshiike.** 1990. Mutational analysis of human papillomavirus type 16 E7 functions. J. Virol. **64**:207–214.

45. **Woodworth, C. D., J. Doniger, and J. A. DiPaolo.** 1989. Immortalization of human foreskin keratinocytes by various human papillomavirus DNAs corresponds to their association with cervical carcinoma. J. Virol. **63**:159–169.

46. **Zorzopulos, J., and L. M. Kazloff.** 1978. Identification of T4D bacteriophage gene product 12 as the baseplate zinc metalloprotein. J. Biol. Chem. **253**:5543–5547.